

Dalton Transactions

Accepted Manuscript



This is an *Accepted Manuscript*, which has been through the Royal Society of Chemistry peer review process and has been accepted for publication.

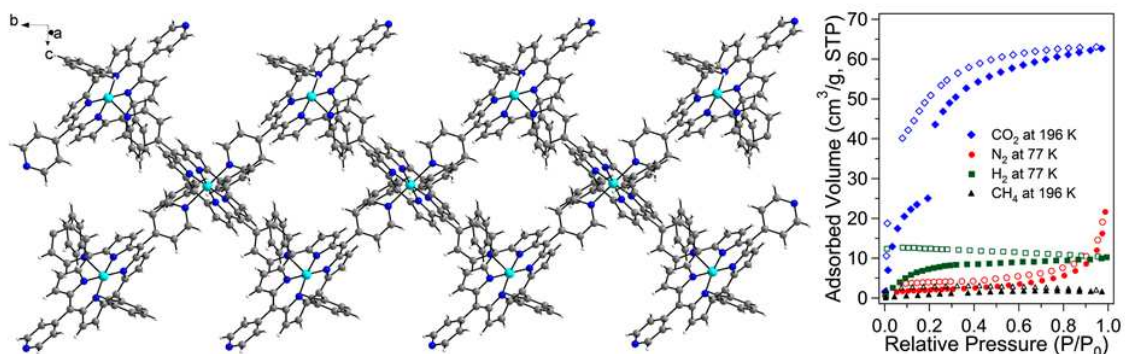
Accepted Manuscripts are published online shortly after acceptance, before technical editing, formatting and proof reading. Using this free service, authors can make their results available to the community, in citable form, before we publish the edited article. We will replace this *Accepted Manuscript* with the edited and formatted *Advance Article* as soon as it is available.

You can find more information about *Accepted Manuscripts* in the [Information for Authors](#).

Please note that technical editing may introduce minor changes to the text and/or graphics, which may alter content. The journal's standard [Terms & Conditions](#) and the [Ethical guidelines](#) still apply. In no event shall the Royal Society of Chemistry be held responsible for any errors or omissions in this *Accepted Manuscript* or any consequences arising from the use of any information it contains.

*Table of Contents***CO₂ selective 1D double chain dipyrindyl-porphyrin based porous coordination polymers†**

Hyun-Chul Kim, Young Sun Lee, Seong Huh, Suk Joong Lee, and Youngmee Kim



Two CO₂ selective 1D double chain dipyrindyl-porphyrin-based porous coordination polymers, M₃(DPyP)₃·4DMF (M = Co, Zn) are prepared from thermal reactions of MnCl(DPyP) with Co^{II} and Zn^{II} ions in DMF.

Cite this: DOI: 10.1039/c0xx00000x

www.rsc.org/xxxxxx

PAPER

CO₂ selective 1D double chain dipyrindyl-porphyrin based porous coordination polymers†

Hyun-Chul Kim,^{a,‡} Young Sun Lee,^{b,‡} Seong Huh,^{*a} Suk Joong Lee,^{*b} and Youngmee Kim^{*c}

Received (in XXX, XXX) Xth XXXXXXXXXX 20XX, Accepted Xth XXXXXXXXXX 20XX

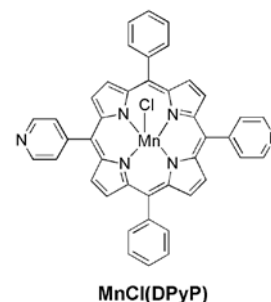
DOI: 10.1039/b000000x

Thermal reactions of MnCl(DPyP) (DPyP = 5,15-di(4-pyridyl)-10,20-diphenylporphyrin) as a metalloligand with Co^{II} and Zn^{II} ions in dimethylformamide led to neutral one-dimensional (1D) double chain dipyrindyl-porphyrin-based porous coordination polymers (PCPs), Co₃(DPyP)₃·4DMF (**I**) and Zn₃(DPyP)₃·2DMF·4H₂O (**II**). Both PCPs were structurally characterized by X-ray crystallography. Particularly, the central Mn^{III} ion in MnCl(DPyP) was transmetallated with Co^{II} or Zn^{II} ions and the central Co^{II} or Zn^{II} ions were further coordinated to pyridyl groups of neighboring M(DPyP) (M = Co or Zn) porphyrin complexes. PCPs **I** and **II** are isostructural and each 1D double chain interacts with another 1D double chain by multiple hydrogen bonding to stabilize the resultant framework. Therefore, solvent-free 1D double chain PCPs have permanent porosity, and the void volumes of the solvent-free **I** and **II** are calculated to be 22.6% and 23.0%, respectively. Gas sorption analysis indicated that **I** and **II** exhibited selective adsorption of CO₂ at 196 K. Both PCPs exhibited much smaller sorption abilities for N₂ (77 K), H₂ (77 K), and CH₄ (196 K) than CO₂ (196 K). Both PCPs exhibited different PXRD patterns when dried at 373 K, which indicated that the framework transformation of the isostructural M₃(DPyP)₃ type of PCPs strongly depended on the type of central metal ions.

1. Introduction

Development of functional porous coordination polymers (PCPs) or metal-organic frameworks (MOFs) is one of the most popular research fields in modern inorganic materials chemistry. Functional PCPs can be utilized for a wide range of applications, including heterogeneous catalysis,¹ CO₂ capture,² H₂ storage,³ and intracellular delivery of small molecules or drugs.⁴ The main strategy to develop new efficient functional PCPs mainly relies on the design of a new polytopic N-donor or carboxylate bridging ligands together with a suitable choice of metal ion.⁵ In fact, numerous examples of new polytopic bridging ligands have expanded the versatility of the resulting functional PCPs into novel applications such as optical sensing,⁶ proton conduction,⁷ charge transport,⁸ and selective encapsulation of guest molecules.⁹

Recently, PCPs containing porphyrin moieties have played a significant role in expanding the development of new functional PCPs. Once porphyrin moieties are successfully incorporated into the framework, versatile applications could be realized because porphyrin units possess various functionalities in catalysis¹⁰ and photon-related applications such as photovoltaics¹¹ and photosensitization.¹² Furthermore, the large molecular size of porphyrin units is adequate for the preparation of robust frameworks with high surface area. Recently, an increasing number of reports have been presented on porphyrin-based PCPs. Wu et al. developed porphyrin carboxylate-based heterometallic PCPs for oxidation and aldol reaction.¹³ Choe et al. reported Zn-tetra-(4-carboxyphenyl)porphyrin PCP for high pressure



Scheme 1. Chemical structure of ditopic metalloligand MnCl(DPyP).

cryogenic H₂ sorption application.¹⁴ Zhang et al. reported on Zn-PCP prepared from 3,5-bis[(4-carboxy)phenyl]phenyl porphyrin and its selective CO₂ sorption over N₂.¹⁵ Ma et al. also prepared Zr-PCP from Fe^{III} metallated tetrakis(4-carboxyphenyl)porphyrin, FeCl(TCPP).¹⁶ Hupp et al. developed very rare biomimetic catalytic systems based on porphyrinic PCPs using metallated porphyrin units.¹⁷

In order to expand the porphyrin-based PCP chemistry, we focused on N-donor based porphyrin molecules such as ditopic 5,15-di(4-pyridyl)-10,20-diphenylporphyrin (DPyP). We attempted to prepare PCPs using a potential metalloligand MnCl(DPyP) as shown in Scheme 1 and divalent transition metal ions including Co^{II} and Zn^{II}. In this report, we describe the reactions between MnCl(DPyP) and Co(NO₃)₂·6H₂O or Zn(NO₃)₂·6H₂O and the resultant permanently microporous CO₂ selective 1D double chain PCPs.

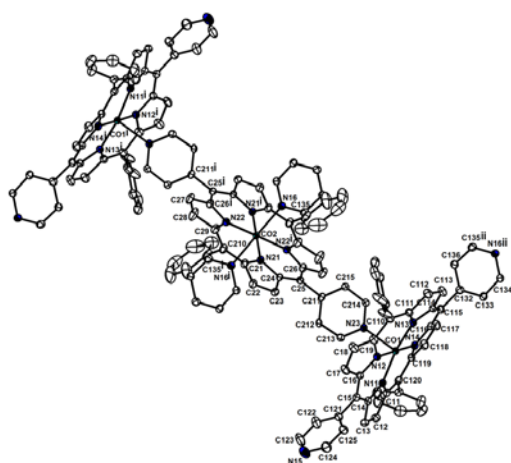


Fig. 1 Formula unit of **I** with atomic labelling scheme. Displacement ellipsoids are shown at the 50% probability level. DMF solvent molecules and all hydrogen atoms were omitted for clarity. Symmetry operations: (i) 1-x, 2-y, 1-z, and (ii) 1-x, 1-y, 1-z.

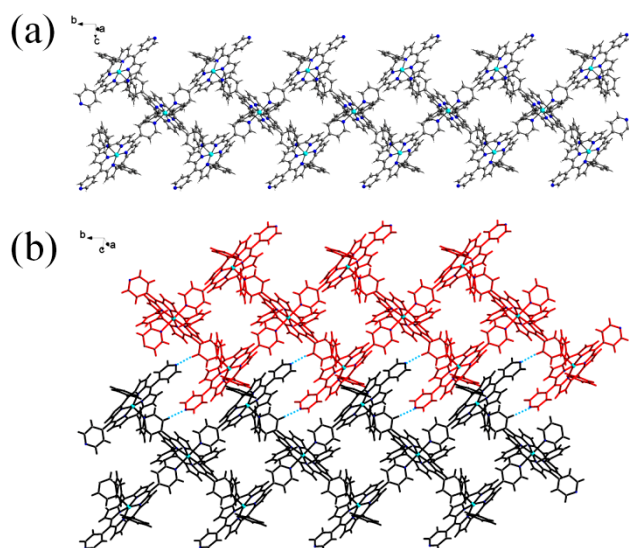


Fig. 2 (a) 1D double chain structure of **I**. All DMF solvent molecules were omitted for clarity. (b) Hydrogen bonds between 1D double chains are shown as green dotted lines. Two 1D double chain coordination polymers are shown as different colors for clarity.

2. Results and discussion

2.1 Structure description

Two metalloporphyrin-based PCPs were obtained using the solvothermal method with DMF solvent. The ligand, DPyP, has a porphyrin core bearing two pyridyl groups with two coordination sites at the 5- and 15-meso positions as shown in Scheme 1. Thus, the molecular symmetry of the free ligand is very similar to the commonly employed ditopic N-donor bridging ligands such as 4,4'-bipyridyl, phenazine, and 1,4-diazabicyclo[2,2,2]octane (DABCO). Reactions between Mn^{III} metalloligand $MnCl(DPyP)$ and divalent transition metal ions such as $Co(NO_3)_2 \cdot 6H_2O$ and $Zn(NO_3)_2 \cdot 6H_2O$ have been conducted in dimethylformamide (DMF) at 120 °C. $MnCl(DPyP)$ was completely transmetallated with Co^{II} or Zn^{II} ions, providing 1D porphyrin-PCPs, $Co_3(DPyP)_3 \cdot 4DMF$ (**I**) or $Zn_3(DPyP)_3 \cdot 2DMF \cdot 4H_2O$ (**II**).

The formula unit of **I** and **II** contains three metal ions, three

porphyrin ligands, and DMF or water solvent molecules as shown in Figs. 1 and S1. The inversion center rides on the middle metal ion, and the two pyridyl nitrogen atoms of the ligand coordinate the neighboring metal ions to provide a 1D double chain as depicted in Figs. 2a and S2a. Unexpectedly, one of the pyridyl groups on the side metallated porphyrins remains uncoordinated, and inter-chain non-classical hydrogen bonds occur between the coordinated pyridyl hydrogen atom and the uncoordinated pyridyl nitrogen atom ($C-H \cdots N$ 2.37(3) Å for **I** and 2.38(4) Å for **II**) (Figs. 2b and S2b). The coordination geometry of the middle metal ion is a distorted octahedral constructed from four pyrrolic nitrogen atoms and two apical pyridyl nitrogen atoms, and that of the side metal ions is a square pyramidal constructed from four pyrrolic nitrogen atoms and one apical pyridyl nitrogen atom. The side metallated porphyrins are considerably distorted from the N4 pyrrolic plane while the middle one is perfectly planar. The angles between the N4 plane and each pyrrolic ring are [10.0°, 13.6°, 11.4°, and 11.5°] for **I** and [8.5°, 9.7°, 8.8°, and 12.2°] for **II**. A Co^{II} ion in **I** is located almost at the centre of the N4 plane, but a Zn^{II} ion in **II** is located a little above the N4 plane with 0.250(4) Å out of the N4 plane. In the packing diagram, the side metallated porphyrins on one chain face the neighboring side one with an $M \cdots M$ distance of 5.278(4) Å for **I** and 5.50(9) Å for **II**.

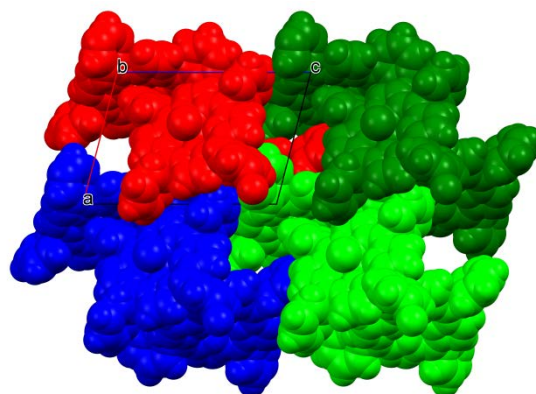


Fig. 3 Space-filling model of four selected 1D double chains for **I** with different colors viewed down the *b*-axis, indicating efficient packing of each chain.

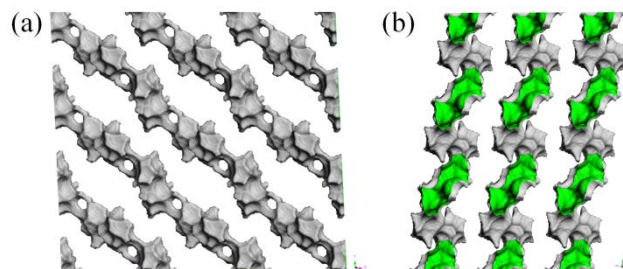


Fig. 4 Isosurface of the channels for solvent-free **I** along the *a*-axis (a) and *c*-axis (b). Grey and green colors indicate the exterior and interior of the isosurface, respectively.

The packing diagrams shown in Figs. 3 and S3 reveal that each 1D double chain tightly packs to form stable solid state structures of **I** and **II**. As depicted in Figs. 4 and S4, both solvent-free **I** and **II** contain well defined open channels. The channels are not cylindrical shape but rather complex undulated geometry. The respective void volumes of the solvent-free **I** and **II** are 22.6%

and 23.0% based on PLATON analysis.¹⁸ Thus, regardless of the type of metal ion, Co^{II} or Zn^{II}, the porosity of **I** and **II** as well as the solid state structures is virtually identical. Interestingly, both PCPs could also be directly synthesized from the reaction of free base DPyP with Co(NO₃)₂·6H₂O or Zn(NO₃)₂·6H₂O in DMF under the same reaction conditions.

2.2 Gas sorption

All solvent molecules in as-prepared **I** and **II** could be completely removed by heating of CHCl₃-exchanged samples at 100 °C under high vacuum based on thermogravimetric analysis (TGA) as shown in Figure S5. In order to probe the gas sorption abilities of evacuated **I** and **II**, standard volumetric gas sorption analyses for N₂, CO₂, H₂, and CH₄ were performed at suitable temperatures as depicted in Fig. 5. Except for CO₂ sorption at 196 K, both **I** and **II** exhibited very low levels of cryogenic gas adsorption for N₂, H₂, and CH₄. For CO₂ sorption of evacuated **I** at 196 K, the adsorption and desorption isotherms gave very similar shapes with slight hysteric behavior, as shown in Fig. 5a. The amount of uptake at 1 atm was 59.0 cm³ g⁻¹ (2.63 mmol g⁻¹). Although the corresponding value for N₂ adsorption at 1 atm was 28.5 cm³ g⁻¹, the adsorption isotherm only starts to exhibit meaningful values of uptake at a higher pressure (> 0.8 atm). The smallest sized H₂ molecules adsorbed more efficiently than the largest sized CH₄. Nevertheless, the value for H₂ adsorption at 1

atm was merely 12.8 cm³ g⁻¹, and this value was much smaller than both CO₂ and N₂. Based on these sorption data, it is obvious that evacuated **I** is a selective sorbent for CO₂.

The evacuated **II** also exhibited very similar trend of gas sorption abilities compared to **I**, as depicted in Fig. 5b. The measured data for CO₂ at 196 K (62.9 cm³ g⁻¹, 2.81 mmol g⁻¹), N₂ at 77 K (21.6 cm³ g⁻¹), H₂ at 77 K (10.2 cm³ g⁻¹), and CH₄ at 196 K (1.6 cm³ g⁻¹) are very close to those of **I**. It is also noted that the adsorption isotherm for CO₂ indicates a more pronounced step at around 0.2 atm than **I**. The sudden increase of CO₂ uptake could be attributable to either the framework transition during CO₂ sorption¹⁹ or electronic attractions between preadsorbed CO₂ molecules and newly adsorbed CO₂ molecules.²⁰ The hysteric behavior between adsorption and desorption isotherms is also slightly larger than **I**.

2.3 Structural transformations

The X-ray crystal structures of the evacuated **I** and **II** could not be obtained due to the loss of single crystallinity. However, powder X-ray diffraction (PXRD) analysis of the evacuated PCPs often provides valuable insights into the framework transformation during activation processes.²¹ Because both **I** and **II** exhibited a noticeable adsorption step for CO₂ adsorption, the PXRD patterns of the evacuated samples were compared with the original structures of the as-prepared PCPs. The PXRD patterns for the as-prepared samples simulated from X-ray crystallographic data and evacuated PCPs are given in Fig. 6. Clearly, the patterns after evacuation differ significantly from those of the as-prepared samples.

For quantitative analysis of these changes, we analyzed the new patterns using DICVOL91.²² The indexed PXRD patterns are also depicted in Fig. 6. The respective calculated unit cell dimensions are a triclinic cell system with $a = 12.1038(160)$ Å, $b = 10.0024(181)$ Å, $c = 18.0586(237)$ Å, $\alpha = 96.877(235)^\circ$, $\beta = 112.040(104)^\circ$, $\gamma = 101.209(228)^\circ$, and $V = 1942.73$ Å³ for **I** and a triclinic cell system with $a = 15.742(207)$ Å, $b = 10.4827(83)$ Å, $c = 25.7512(347)$ Å, $\alpha = 90.564(85)^\circ$, $\beta = 131.846(100)^\circ$, $\gamma = 104.095(74)^\circ$, and $V = 2981.55$ Å³ for **II**. The corresponding figures of merit for **I** are $M_{19}^{23} = 7.5$ and $F_{19}^{24} = 13.6$, while the values for **II** are $M_{20}^{23} = 9.7$ and $F_{20}^{24} = 21.4$. It is worth noting that the unit cell dimensions of both PCPs had significantly changed compared to their original cell dimensions. The unit cell dimensions of b -axis for **I** and **II** are reduced to around 10 Å from 14.7137(4) Å and 14.960(3) Å. On the other hand, the dimensional changes of a - and c -axes indicated clear differences between **I** and **II**. In **I**, the a -axis dimension slightly increased from 11.8046(3) Å to 12.1038(160) Å. However, the a -axis of **II** was increased significantly from 11.840(2) Å to 15.7412(207) Å. In the cases of c -axis, **I** exhibited a slight increase from 16.5306(5) Å to 18.0586(237) Å, while **II** showed a pronounced increase from 16.671(3) Å to 25.7512(347) Å. The resultant unit cell volume changes are more remarkable. The cell volume for **I** decreased from 2744.14 Å³ to 1942.73 Å³. In contrast, the cell volume for **II** increased from 2822.6 Å³ to 2981.55 Å³. These results clearly suggest that the effects of different metal ions in the isostructural porphyrin-based PCPs are rather high for structural changes during activation processes.

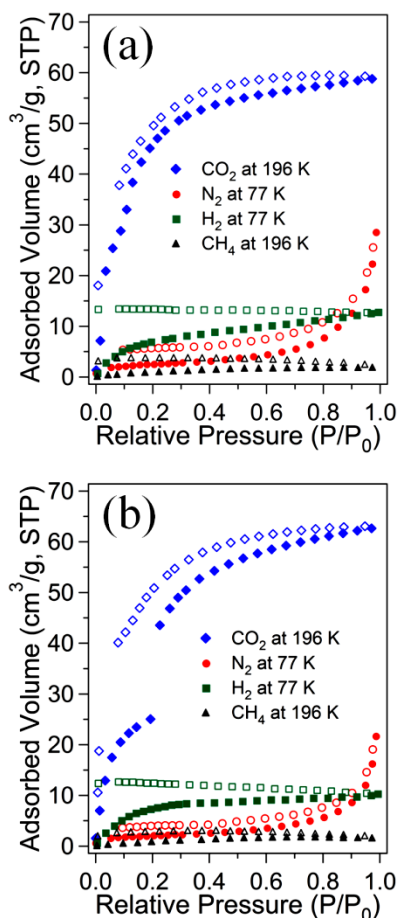


Fig. 5 Cryogenic gas adsorption-desorption isotherms for CO₂, N₂, H₂, and CH₄ for evacuated **I** (a) and **II** (b). Solid symbols and open symbols represent the adsorption and desorption isotherms, respectively.

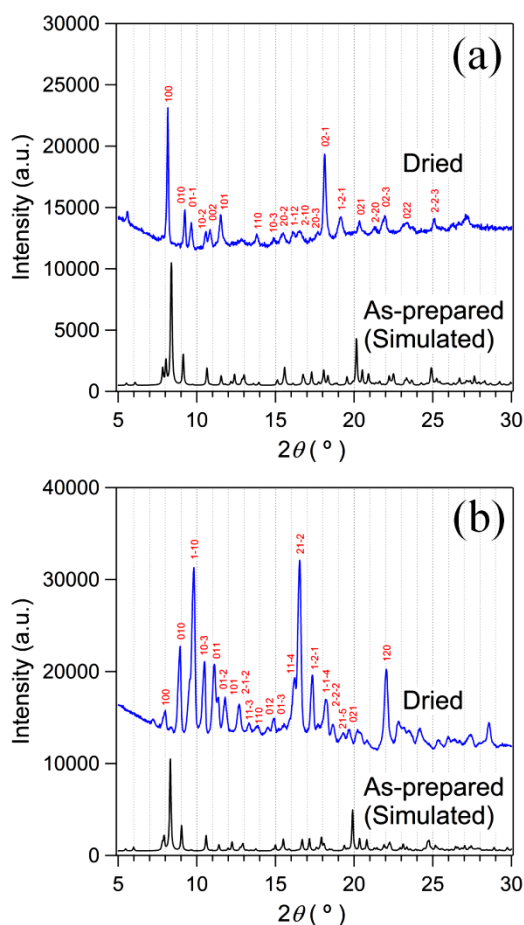


Fig. 6 Comparison of the PXRD patterns of the simulated (= as-prepared) data from X-ray crystallography and dried samples: **I** (a) and **II** (b). The indexing of the PXRD patterns for the dried samples was performed using DICVOL91.

3. Conclusions

Thermal reactions of a potential ditopic metalloligand $\text{MnCl}(\text{DPyP})$ with Co^{II} or Zn^{II} ions in DMF afforded two one-dimensional (1D) double chain dipyrrolyl-porphyrin based porous coordination polymers (PCPs), $\text{Co}_3(\text{DPyP})_3 \cdot 4\text{DMF}$ (**I**) and $\text{Zn}_3(\text{DPyP})_3 \cdot 2\text{DMF} \cdot 4\text{H}_2\text{O}$ (**II**). The two PCPs were completely isostructural, based on a single crystal X-ray diffraction analysis. In both cases, transmetallation occurred during the reactions. Both evacuated **I** and **II** were permanently porous with adsorption selectivity for CO_2 over N_2 , H_2 , and CH_4 at low temperature and low pressure. Their CO_2 uptake levels were almost identical at 196 K. Judging from the PXRD patterns for evacuated **I** and **II**, the framework structures of both PCPs showed significant differences after the evacuation of DMF solvate molecules. Also, both transformed structures changed from their original framework structures. It is worth noting that the framework stability is strongly dependent on the central metal ions, even for the isostructural porphyrin-based PCPs.

4. Experimental

Materials

Meso-Phenyldipyrromethane, 5,15-di(4-pyridyl)-10,20-diphenylporphyrin (DPyP), and [5,15-di(4-pyridyl)-10,20-diphenyl-

porphyrinato]manganese(III) chloride ($\text{MnCl}(\text{DpyP})$) were synthesized according to modified procedures outlined in the literature.²⁵ All other chemicals were obtained from commercial sources and used without further purification. All of the reactions and manipulations of the porphyrin building blocks were carried out under N_2 with the use of standard inert-atmosphere and Schlenk techniques, unless otherwise noted. The solvents used in inert-atmosphere reactions were dried and degassed using standard procedures. Flash column chromatography was carried out with 230-400 mesh silica gel from Sigma-Aldrich using a wet-packing method. All deuterated solvents were purchased from Cambridge Isotope Laboratory.

Instrumentation

The cryogenic N_2 adsorption-desorption analysis was performed on a Belsorp-miniII at 77 K (BEL Japan). The CHCl_3 -exchanged porphyrin-PCPs were dried at 373 K for 2 h under high vacuum before measurements were taken. Low pressure CO_2 adsorption measurements were taken on the same equipment at 196 K (2-propanol/dry ice bath), 273 K (ice bath), and 298 K (water bath). Low-pressure hydrogen and methane adsorption measurements were performed at 77 K and 196 K, respectively, on the same equipment. Powder X-ray diffraction patterns were obtained using a Bruker D8 Advance diffractometer (40 kV, 40 mA, step size = 0.02°). NMR spectra were recorded on a Varian AS400 (399.937 MHz for ^1H and 100.573 MHz for ^{13}C) spectrometer. ^1H chemical shifts are referenced to the proton resonance resulting from protic residue in deuterated solvent and the ^{13}C chemical shift recorded downfield in ppm relative to the carbon resonance of the deuterated solvents. Absorbance and emission spectra were obtained using an Agilent UV-Vis-NIR spectrophotometer with quartz cells. Matrix-Assisted Laser-Desorption-Ionization Time-of-flight Mass Spectra (MALDI-TOF) were obtained on a Bruker Daltonics LRF20 MALDI-TOF Mass Spectrometer at the Industry-Academic Cooperation Foundation, Yonsei University. ICP-AES data were obtained at Korea Basic Science Institute. Elemental analyses were performed on Thermo FLASH1112 Elemental analyzer at the Elemental Analysis Service Centre of Sogang University, Korea. Thermogravimetric analysis was carried out on a TGA Q5000 (TA Instruments) under a nitrogen atmosphere (ramping rate = $15^\circ\text{C min}^{-1}$).

5,15-di(4-pyridyl)-10,20-diphenylporphyrin (DPyP): *meso*-phenyldipyrromethane (1.0 g, 4.4 mmol) and 4-pyridine-carboxaldehyde (0.42 mL, 4.4 mmol) were dissolved in propionic acid (38 mL) in a 100-mL round-bottom flask equipped with a magnetic stir bar and a water-cooled reflux condenser. The mixture was then allowed to reflux for 2 h under air. After cooling to room temperature, the reaction mixture was evaporated until dry using a rotary evaporator to yield a dark residue, which was dissolved in dichloromethane. The mixture was washed with saturated K_2CO_3 (0.1 M) and water (50 mL), dried over anhydrous MgSO_4 , and concentrated until dry using a rotary evaporator. The resulting residue was purified by silica-gel column chromatography (tetrahydrofuran/dichloromethane, 1:9 v/v). After recrystallization from dichloromethane and methanol, a pure product was obtained as a purple solid (0.106 g, 8%). ^1H NMR (CDCl_3 , ppm): δ 12.13 (s, 2H), 9.04 (d, $^3J_{\text{H-H}} = 6.26$ Hz, 4H), 8.90 (d, $^3J_{\text{H-H}} = 4.49$ Hz, 4H), 8.80 (d, $^3J_{\text{H-H}} = 4.69$ Hz, 4H),

8.20 (*d*, $^3J_{\text{H-H}} = 6.26$ Hz, 4H), 8.17 (*d*, $^3J_{\text{H-H}} = 6.26$ Hz, 4H), 7.70 (*m*, 6H). ^{13}C NMR (CDCl_3 , ppm): δ 148.924, 132.351, 124.513, 121.392, 101.354, 94.142, 90.891, 31.721, 31.024, 28.962, 23.216, 13.863. MS (MALDI-TOF): $m/z = 617.262$ for M^+ ; Calcd 616.71.

[5,15-di(4-pyridyl)-10,20-diphenylporphyrinato]-manganese(III) chloride (MnCl(DPyP)): A solution of DPyP (0.250 g, 0.41 mmol) and $\text{MnCl}_2 \cdot 4\text{H}_2\text{O}$ (0.811 g, 4.10 mmol) in DMF (12.5 mL) was heated to reflux for 6 h. The reaction was monitored using UV-Vis spectroscopy. The reaction mixture was allowed to cool to room temperature and DMF was then evaporated under reduced pressure. The resulting residue was then dispersed in water, filtered and dried in a high vacuum. The crude product was purified by column chromatography (methanol/dichloromethane, 1:9 v/v). After recrystallization from dichloromethane, methanol and THF, a pure product was obtained as a dark solid (0.260 g, 90%). MS (MALDI-TOF): $m/z = 669.734$ for $[\text{M}-\text{Cl}]^+$; Calcd 669.63. Anal. Calcd. for $\text{C}_{42}\text{H}_{26}\text{N}_6\text{MnCl} \cdot \text{THF}$ (777.19): C, 71.09; H, 4.41; N, 10.81. Found: C, 71.12; H, 5.11; N, 11.15.

Preparation of $\text{Co}_3(\text{DPyP})_3 \cdot 4\text{DMF}$ (I): $\text{MnCl}(\text{DPyP})$ (0.070 g, 0.1 mmol), $\text{Co}(\text{NO}_3)_2 \cdot 6\text{H}_2\text{O}$ (0.029 g, 0.1 mmol), and DMF (5 mL) were placed in a Teflon-lined high pressure bomb. The bomb was placed in an oven at 120 °C for 48 h. After cooling to room temperature, the purple crystalline solids were recovered and washed with DMF and air-dried. The yield was 0.062 g (81%). Single crystals suitable for X-ray crystallography were directly chosen from the as-prepared crystals. ICP data shows the starting Mn ions were exchanged to Co ions (Table S1). Anal. Calcd. for $\text{C}_{138}\text{H}_{106}\text{N}_{22}\text{O}_4\text{Co}_3$ (2313.26): C, 71.65; H, 4.62; N, 13.32. Found: C, 71.17; H, 4.74; N, 13.23.

Preparation of $\text{Zn}_3(\text{DPyP})_3 \cdot 2\text{DMF} \cdot 4\text{H}_2\text{O}$ (II): $\text{MnCl}(\text{DPyP})$ (0.070 g, 0.1 mmol), $\text{Zn}(\text{NO}_3)_2 \cdot 6\text{H}_2\text{O}$ (0.030 g, 0.1 mmol), and DMF (5 mL) were placed in a Teflon-lined high pressure bomb. The bomb was placed in an oven at 120 °C for 72 h. After cooling to room temperature, the very large purple crystals were recovered and washed with DMF and air-dried. The yield was 0.033 g (42%). Single crystals suitable for X-ray crystallography were directly chosen from the as-prepared crystals. Anal. Calcd. for $\text{C}_{132}\text{H}_{100}\text{N}_{20}\text{O}_6\text{Zn}_3$ (2258.51): C, 70.20; H, 4.46; N, 12.40. Found: C, 70.71; H, 4.65; N, 11.37.

X-ray crystallography: The X-ray diffraction data for **I** and **II** were collected on a Bruker SMART APEX diffractometer equipped with a monochromator in a Mo $\text{K}\alpha$ ($\lambda = 0.71073$ Å) incident beam. Each crystal was mounted on a glass fiber. The CCD data were integrated and scaled using the Bruker-SMART software package, and the structure was solved and refined using SHELXTL V6.12. All hydrogen atoms were placed in the calculated positions. The crystallographic data for PCPs **I** and **II** are listed in Table 1. The selected bond distances are listed in Table 2. Structural information was deposited at the Cambridge Crystallographic Data Centre (CCDC reference numbers are 948353 for **I** and 948354 for **II**).

Acknowledgments

The Basic Science Research Program through the National Research Foundation of Korea (NRF) funded by the Ministry of Education, Science and Technology (20110008018, 2013R1A1A2006914, 2013R1A1A2007429 and 20100020209) and the RP-Grant 2013 of Ewha Womans University are gratefully acknowledged.

Table 1. Crystallographic Data for **I** and **II**.

	I	II
Empirical formula	$\text{C}_{132}\text{H}_{92}\text{N}_{20}\text{O}_2\text{Co}_3$	$\text{C}_{132}\text{H}_{92}\text{N}_{20}\text{O}_2\text{Zn}_3$
Formula weight	2167.05	2186.37
Temperature (K)	170(2)	170(2)
Wavelength (Å)	0.71073	0.71073
Space group	P-1	P-1
a (Å)	11.898(2)	11.840(2)
b (Å)	14.656(3)	14.960(3)
c (Å)	16.595(3)	16.671(3)
α (°)	90.03(3)	90.42(3)
β (°)	104.37(3)	104.33(3)
γ (°)	98.74(3)	99.00(3)
Volume(Å ³)	2768.5(10)	2822.6(10)
Z	1	1
Density (calc.) (Mg/m ³)	1.300	1.286
Absorption coeff. (mm ⁻¹)	0.508	0.695
Crystal size (mm ³)	0.36 x 0.10 x 0.04	0.12 x 0.10 x 0.10
Reflections collected	14201	15881
Independent reflections	9458 [R(int) = 0.0418]	10726 [R(int) = 0.0450]
Data / restraints / parameters	9458 / 68 / 734	10726 / 66 / 758
Goodness-of-fit on F ²	0.992	1.049
Final R indices	$R_1 = 0.0704$, $wR_2 = 0.1826$	$R_1 = 0.0684$, $wR_2 = 0.1845$
R indices (all data)	$R_1 = 0.1117$, $wR_2 = 0.2061$	$R_1 = 0.0815$, $wR_2 = 0.1965$
Largest diff. peak and hole (e.Å ⁻³)	1.427 and -0.472	1.849 and -0.556

Table 2. Selected Bond Distances for **I** and **II**.

	I	II
M-N _{pyrrole} (Å)	1.965(4)-2.007(4)	2.049(3)-2.175(3)
M-N _{py} (Å)	2.178(4), 2.288(4)	2.384(3)

Notes and references

- ^aDepartment of Chemistry and Protein Research Center for Bio-Industry, Hankuk University of Foreign Studies, Yongin 449-791, Republic of Korea. Fax: +82 31 330 4566; Tel: +82 31 330 4522; E-mail: shuh@hufs.ac.kr
- ^bDepartment of Chemistry, Research Institute for Natural Sciences, Korea University, Seoul 136-701, Korea. Fax: +82-2-924-3141; E-mail: slee1@korea.ac.kr
- ^cDepartment of Chemistry and Nano Science, Institute of Nano-Bio Technology, Ewha Womans University, Seoul 120-750, Republic of Korea. Fax: +82 2 3277 3419; Tel: +82 2 3277 4164; E-mail: ymeekim@ewha.ac.kr
- [†]Electronic Supplementary Information (ESI) available: crystal structures and packing diagram of **II** and isosurface of solvent-free **II**. ICP-AES data, TGA
- [‡]These authors contributed equally to this work.
- 85 1 (a) M. Fujita, Y. J. Kwon, S. Washizu and K. Ogura, *J. Am. Chem. Soc.*, 1994, **116**, 1151; (b) S. J. Lee, A. Hu and W. Lin, *J. Am. Chem. Soc.*, 2002, **124**, 12948; (c) K. Schlichte, T. Kratzke and S. Kaskel, *Micropor. Mesopor. Mater.*, 2004, **73**, 81; (d) S. Horike, M. M.

- Dincă, K. Tamaki and J. R. Long, *J. Am. Chem. Soc.*, 2008, **130**, 5854; (e) A. M. Shultz, O. K. Farha, J. T. Hupp and S. T. Nguyen, *J. Am. Chem. Soc.*, 2009, **131**, 4204; (f) K. Oisaki, Q. Li, H. Furukawa, A. U. Czaja and O. M. Yaghi, *J. Am. Chem. Soc.*, 2010, **132**, 9262; (g) S. Bhattacharjee, D.-A. Yang and W.-S. Ahn, *Chem. Commun.*, 2011, **47**, 3637; (h) D. J. Lun, G. I. N. Waterhouse and S. G. Telfer, *J. Am. Chem. Soc.*, 2011, **133**, 5806; (i) J.-M. Gu, W.-S. Kim and S. Huh, *Dalton Trans.*, 2011, **40**, 10826; (j) I. H. Hwang, J. M. Bae, W.-S. Kim, Y. D. Jo, C. Kim, Y. Kim, S.-J. Kim and S. Huh, *Dalton Trans.*, 2012, **41**, 12759; (k) W.-S. Kim, K. Y. Lee, E.-H. Ryu, J.-M. Gu, Y. Kim, S. J. Lee and S. Huh, *Eur. J. Inorg. Chem.*, 2013, 4228.
- 2 (a) R. Banerjee, A. Phan, B. Wang, C. Knobler, H. Furukawa, M. O’Keeffe and O. M. Yaghi, *Science*, 2008, **319**, 939; (b) G. Férey, *Chem. Soc. Rev.*, 2008, **37**, 191; (c) D. Britt, H. Furukawa, B. Wang, T. G. Glover and O. M. Yaghi, *Proc. Natl. Acad. Sci. U. S. A.*, 2009, **106**, 20637; (d) H. Furukawa and O. M. Yaghi, *J. Am. Chem. Soc.*, 2009, **131**, 8875; (e) A. R. Millward and O. M. Yaghi, *J. Am. Chem. Soc.*, 2005, **127**, 17998; (f) S. R. Caskey, A. G. Wong-Foy and A. J. Matzger, *J. Am. Chem. Soc.*, 2008, **130**, 10870; (g) Y.-S. Bae, O. K. Farha, J. T. Hupp and R. Q. Snurr, *J. Mater. Chem.*, 2009, **19**, 2131; (h) Y.-S. Bae, O. K. Farha, A. M. Spokoynny, C. A. Mirkin, J. T. Hupp and R. Q. Snurr, *Chem. Commun.*, 2008, 4135; (i) A. U. Czaja, N. Trukhan and U. Müller, *Chem. Soc. Rev.*, 2009, **38**, 1284; (j) J.-R. Li, R. J. Kuppler and H.-C. Zhou, *Chem. Soc. Rev.*, 2009, **38**, 1477; (k) J.-M. Gu, T.-H. Kwon, J.-H. Park and S. Huh, *Dalton Trans.*, 2010, **39**, 5608; (l) K. Sumida, D. L. Rogow, J. A. Mason, T. M. McDonald, E. D. Bloch, Z. R. Herm, T.-H. Bae and J. R. Long, *Chem. Rev.*, 2012, **112**, 724; (m) I. H. Hwang, H.-Y. Kim, M. M. Lee, Y. J. Na, J. H. Kim, H.-C. Kim, C. Kim, S. Huh, Y. Kim and S.-J. Kim, *Cryst. Growth Des.*, 2013, **13**, 4815; (n) Q. Chen, Z. Chang, W.-C. Song, H. Song, H.-B. Song, T.-L. Hu and X.-H. Bu, *Angew. Chem. Int. Ed.* 2013, **52**, 11550; (o) J.-R. Li, Y. Tao, Q. Yu, X.-H. Bu, H. Sakamoto and S. Kitagawa, *Chem. Eur. J.* 2008, **14**, 2771; (p) S.-M. Zhang, Z. Chang, T.-L. Hu and X.-H. Bu, *Inorg. Chem.* 2010, **49**, 11581.
- 35 (a) M. Eddaoudi, D. B. Moler, H. Li, B. Chen, T. M. Reineke, M. O’Keeffe and O. M. Yaghi, *Acc. Chem. Res.*, 2001, **34**, 319; (b) J. L. C. Rowsell and O. M. Yaghi, *Angew. Chem., Int. Ed.*, 2005, **44**, 4670; (c) D. J. Collins and H.-C. Zhou, *J. Mater. Chem.*, 2007, **17**, 3154; (d) M. Dincă and J. R. Long, *Angew. Chem., Int. Ed.*, 2008, **47**, 6766; (e) J. Germain, J. M. J. Fréchet and F. Svec, *Small*, 2009, **5**, 1098; (f) M. Hirscher, *Angew. Chem., Int. Ed.*, 2011, **50**, 581; (g) T. Hügle, M. Hartl and D. Lentz, *Chem. Eur. J.*, 2011, **17**, 10184.
- 4 (a) J. An, S. J. Geib and N. L. Rosi, *J. Am. Chem. Soc.*, 2009, **131**, 8376; (b) P. Horcajada, T. Chalati, C. Serre, B. Gillet, C. Sebrie, T. Baati, J. F. Eubank, D. Heurtaux, P. Clayette, C. Kreuz, J.-S. Chang, Y. K. Hwang, V. Marsaud, P.-N. Bories, L. Cynober, S. Gil, G. Férey, P. Couvreur and R. Gref, *Nat. Mater.*, 2010, **9**, 172; (c) L. Xing, Y. Cao and S. Che, *Chem. Commun.*, 2012, **48**, 5995; (d) A. C. McKinlay, J. F. Eubank, S. Wuttke, B. Xiao, P. S. Wheatley, P. Bazin, J.-C. Lavalley, M. Daturi, A. Vimont, G. De Weireld, P. Horcajada, C. Serre and R. E. Morris, *Chem. Mater.*, 2013, **25**, 1592; (e) D. Cunha, M. B. Yahia, S. Hall, S. R. Miller, H. Chevreau, E. Elkaim, G. Maurin, P. Horcajada and C. Serre, *Chem. Mater.*, 2013, **25**, 2767; (f) M. Ma, H. Noei, B. Mienert, J. Niesel, E. Bill, M. Muhler, R. A. Fischer, Y. Wang, U. Schatzschneider and N. Metzler-Nolte, *Chem. Eur. J.*, 2013, **19**, 6785.
- 5 (a) O. M. Yaghi, M. O’Keeffe, N. W. Ockwig, H. K. Chae, M. Eddaoudi and J. Kim, *Nature*, 2003, **423**, 705; (b) H. Furukawa, K. E. Cordova, M. O’Keeffe and O. M. Yaghi, *Science*, 2013, **341**, 1230444.
- 6 (a) H.-L. Jiang, Y. Tatsu, Z.-H. Lu and Q. Xu, *J. Am. Chem. Soc.*, 2010, **132**, 5586; (b) Z.-Z. Lu, R. Zhang, Y.-Z. Li, Z.-J. Guo and H.-G. Zheng, *J. Am. Chem. Soc.*, 2011, **133**, 4172; (c) S. Pramanik, C. Zheng, X. Zhang, T. J. Emge and J. Li, *J. Am. Chem. Soc.*, 2011, **133**, 4153.
- 7 (a) A. Shigematsu, T. Yamada and H. Kitagawa, *J. Am. Chem. Soc.*, 2011, **133**, 2034; (b) T. Kundu, S. C. Sahoo and R. Banerjee, *Chem. Commun.*, 2012, **48**, 4998; (c) T. Panda, T. Kundu and R. Banerjee, *Chem. Commun.*, 2012, **48**, 5464; (d) G. K. H. Shimizu, J. M. Taylor, S. R. Kim, *Science*, 2013, **341**, 354; (e) J. M. Taylor, K. W. Dawson and G. K. H. Shimizu, *J. Am. Chem. Soc.*, 2013, **135**, 1193.
- 8 T. C. Narayan, T. Miyakai, S. Seki and M. Dincă, *J. Am. Chem. Soc.*, 2012, **134**, 12932.
- 9 (a) Q. Li, W. Zhang, O. Š. Miljanić, C.-H. Sue, Y.-L. Zhao, L. Liu, C. B. Knobler, J. F. Stoddart and O. M. Yaghi, *Science*, 2009, **325**, 855; (b) K. Kim, *Nat. Chem.*, 2009, **1**, 603.
- 10 J. Poltowicz, E. M. Serwicka, E. Bastardo-Gonzalez, W. Jones and R. Mokaya, *Appl. Catal. A: General*, 2001, **218**, 211.
- 11 A. Yella, H.-W. Lee, H. N. Tsao, C. Yi, A. K. Chandiran, Md.K. Nazeeruddin, E. W.-G. Diau, C.-Y. Yeh, S. M. Zakeeruddin and M. Grätzel, *Science*, 2011, **334**, 629.
- 12 F. Figueira, J. A. S. Cavaleiro and J. P. C. Tomé, *J. Porphy. Phthalocya.*, 2011, **15**, 517.
- 13 C. Zou, T. Zhang, M.-H. Xie, L. Yan, G.-Q. Kong, X.-L. Yang, A. Ma and C.-D. Wu, *Inorg. Chem.*, 2013, **52**, 3620.
- 14 E.-Y. Choi, C. A. Wray, C. Hu and W. Choe, *CrystEngComm*, 2009, **11**, 553.
- 15 J. A. Johnson, Q. Lin, L.-C. Wu, N. Obaidi, Z. L. Olson, T. C. Reeson, Y.-S. Chen and J. Zhang, *Chem. Commun.*, 2013, **49**, 2828.
- 16 Y. Chen, T. Hoang and S. Ma, *Inorg. Chem.*, 2012, **51**, 12600.
- 17 O. K. Farha, A. M. Shultz, A. A. Sarjeant, S. T. Nguyen and J. T. Hupp, *J. Am. Chem. Soc.*, 2011, **133**, 5652.
- 18 A. L. Spek, *PLATON-A multipurpose Crystallographic Tool*, Utrecht University, Utrecht, The Netherlands, 2004.
- 19 (a) D. Li and K. Kaneko, *Chem. Phys. Lett.*, 2001, **335**, 50; (b) S. Bourrelly, P. L. Llewellyn, C. Serre, F. Millange, T. Loiseau and G. Férey, *J. Am. Chem. Soc.*, 2005, **127**, 13519.
- 20 K. S. Walton, A. R. Millward, D. Dubbeldam, H. Frost, J. J. Low, O. M. Yaghi and R. Q. Snurr, *J. Am. Chem. Soc.*, 2008, **130**, 406.
- 21 I. H. Hwang, J. M. Bae, Y.-K. Hwang, H.-Y. Kim, C. Kim, S. Huh, S.-J. Kim and Y. Kim, *Dalton Trans.*, 2013, **42**, 15645.
- 22 A. Boultif and D. Louër, *J. Appl. Crystallogr.*, 1991, **24**, 987.
- 23 P. M. de Wolff, *J. Appl. Crystallogr.*, 1968, **1**, 108.
- 24 G. S. Smith and R. L. Snyder, *J. Appl. Crystallogr.*, 1979, **12**, 60.
- 25 (a) E. H. Cho, S. H. Chae, S. J. Lee and J. Joo, *Synth. Met.*, 2012, **162**, 813; (b) D. A. Jose, A. D. Shukla, G. Ramakrishna, D. K. Palit, H. N. Ghosh and A. Das, *J. Phys. Chem. B*, 2007, **111**, 9078; (c) D. H. Lee, S. Kim, M. Y. Hyun, J.-Y. Hong, S. Huh, C. Kim and S. J. Lee, *Chem. Comm.*, 2012, **48**, 5512.